Chemosphere 344 (2023) 140430

Contents lists available at ScienceDirect

Chemosphere

journal homepage: www.elsevier.com/locate/chemosphere

Humic acids on fire? Physico-chemical, thermal, flammability features and extraction process of different humic acids in support of their possible applications

Virginia Venezia [a,b], Maria Portarapillo [a,*], Gianluigi De Falco [a], Roberto Sanchirico [c], Giuseppina Luciani [a], Almerinda Di Benedetto [a]

[a] Dipartimento di Ingegneria Chimica, dei Materiali e della Produzione Industriale, Università degli Studi di Napoli Federico II, P.le Tecchio 80, 80125, Napoli, Italy
[b] Dipartimento di Strutture per l'Ingegneria e l'Architettura, Università degli Studi di Napoli Federico II, Via Claudio 21, 80125, Napoli, Italy
[c] Istituto di Scienze e Tecnologie per l'Energia e la Mobilità Sostenibili, Consiglio Nazionale delle Ricerche (STEMS-CNR), Piazzale V. Tecchio 80, 80125, Napoli, Italy

HIGHLIGHTS

- Flammability, thermal and physico-chemical characterization of HA extracted from three bio-residues was performed.
- Results suggest that HA resilience degree depend on the nature and on the extraction process of the humic acid.
- HA extraction processes affect the nature and the content of their functional groups, changing their application field.
- Aldrich_HA and Compost_HA can be used as flame retardant additives in epoxy systems due to their higher thermal resilience.
- Artichoke_HA and CompostPD_HA can be used as additives for anti-oxidant/microbial films due to their higher reactivity.

GRAPHICAL ABSTRACT

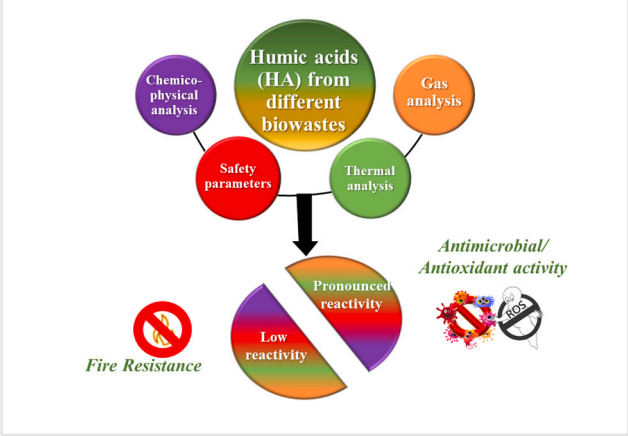

ARTICLE INFO

Handling Editor: X. Cao

Keywords:
Biowaste
Humic acids
Resilience degree
Thermal and fire hazards
Physico-chemical behavior

ABSTRACT

Humic acids (HA) consist in a multitude of heterogeneous organic molecules surviving the biological and chemical degradation of both vegetal and animal biomasses. The great abundance and chemical richness of these residues make their valorisation one of the most promising approaches to move towards a circular economy. However, the heterogeneity of the biomass from which HA are extracted, as well as the production process, significantly affects the nature and the relative content of functional groups (i.e. quinones, phenols and carboxylic and hydroxyl moieties), eventually changing HA reactivity and ultimately determining their application field. Indeed, depending on their properties, these substances can be used as flame retardants in the case of pronounced resilience degree (i.e., absent or low reactivity), or as antioxidant or antimicrobial agents in the case of pronounced reactivity, thanks to their redox behaviour.

* Corresponding author.
E-mail address: maria.portarapillo@unina.it (M. Portarapillo).

https://doi.org/10.1016/j.chemosphere.2023.140430
Received 6 June 2023; Received in revised form 6 October 2023; Accepted 10 October 2023
Available online 11 October 2023
0045-6535/© 2023 The Authors. Published by Elsevier Ltd. This is an open access article under the CC BY license (http://creativecommons.org/licenses/by/4.0/).

In this work we investigated the flammable, the thermal and the physico-chemical features of HA extracted from different composted biomasses to identify the reactivity or the resiliency of these moieties. Several techniques, including flammability characterization (LIT and MIE), laser diffraction granulometry, TG, XRD analyses, FTIR spectroscopy on both solid and gaseous phases, and Raman spectroscopy were integrated to investigate the correlation among the safety parameters, the distributions of particle sizes, as well as the thermal, the chemical properties of HA powders and the influence of post-extraction processes on HA final properties.

1. Introduction

Biowaste (BW) is a rich source of chemical and biological substances and can be converted into added-value compounds and materials through recycling or transformation (B. Xu et al., 2019; C. Xu et al., 2019a). Due to the enormous amount of bio-residues generated by biogenic and non-biogenic transformations, biowaste valorisation is one of the most important issues for sustainable development (C. Xu et al., 2019b).

Biowastes include humic acids (HA), the alkali-soluble fraction of natural organic matter normally found in water, soil, and sediments (Luo et al., 2019; Spaccini et al., 2019). They are formed during the biological and chemical transformation of biomass through natural transformations and are massive by-products in biorefinery processes. HA are heterogeneous mixtures of relatively small molecules (<1000 Da) rich in functional groups such as quinone, phenol, carboxyl and hydroxyl groups that confer them many useful properties including absorption of organic pollutants, chelation of metal ions and regenerable red-ox behavior in terms of antioxidant, antimicrobial and anti-inflammatory activity (Afzal et al., 2019; de Melo et al., 2016; Lowell et al., 2004; Nuzzo et al., 2020; Piccolo, 2002). Moreover, these compounds form supramolecular aggregates stabilised by non-covalent interactions, containing both hydrophobic and hydrophilic domains, thus exhibiting an intrinsic amphiphilic behavior (Ke et al., 2021). Therefore, HA are expected to play a leading role on the green chemistry stage as a cost-effective source for the design and development of multifunctional materials for a variety of applications (de Melo et al., 2016; Venezia et al., 2021, 2022a, 2022b; Vitiello et al., 2021). Indeed, in the case of pronounced resilience degree, these organic moieties can be used as effective flame retardants for polymer systems, mainly thanks to the improvement of thermal stability through the charring process (Liu et al., 2020; Venezia et al., 2021). On the other hand, they can be used as antioxidant or antimicrobial agents in different fields including medicine, sensing, packaging, and environmental remediation (de Melo et al., 2016; Venezia et al., 2022b, 2023). The broad range of functional features, changing from high resilience to prompt red-ox activity, prove the heterogeneous nature of these complex biomolecules. On one side it promotes scientific interest towards their valorisation, on the other it stands as the main limitation to their full technological exploitation.

To this regard, the heterogeneity of the biomass from which HA are extracted, as well as their production process, significantly affect the nature and content of their functional groups, influencing the reactivity and the resilience degree of HA, as well as their effective valorisation procedures.

Therefore, a safety assessment of these complex organic systems is imperative. To the best of our knowledge, there is no insight into the safety aspects of HA processing and handling. Muralidhara et al. (2018) (Muralidhara et al., 2018) showed that the overall fire risk associated with HA is not significantly different from that of conventional fires using more conventional cellulosic fuels. For this reason, further work is needed to gain a more comprehensive understanding of the safety aspects associated with HA use and processing, taking into account the different composition and properties, which are related to both HA origin and extraction methods (Muralidhara et al., 2018).

At the same time, the correlation of thermal and physico-chemical features of HA and their resilient behavior could be crucial to exploit their potential as flame retardancy additives or as redox materials.

In a recent work, we highlighted the importance of a complete chemical-physical and thermal screening of any combustible dust in order to fully understand the explosive behavior in terms of flame propagation pathways and consequently in terms of flammability/explosion parameters (Centrella et al., 2020; Danzi et al., 2023; Danzi et al., 2021; Portarapillo et al., 2020, 2021, 2022). In addition, this approach has been applied to non-traditional powders such as nylon and biomass powders to understand the main flame propagation pathways and the geometrical, chemical, physical and thermal characteristics that most influence the dust dispersion (Portarapillo et al., 2021) and this propagation (Danzi et al., 2021; Portarapillo et al., 2021, 2022).

Inspired by these previous studies, in this work we investigated the flammable, thermal and physicochemical properties of HA from different bio-residues in order to determine the reactivity or resiliency degree of these components, thus getting information about the best possible application of humic acids. For this purpose, a combined approach of several techniques, including flammability characterisation (evaluation of the layer ignition temperature and minimum ignition energy), laser diffraction granulometry, TG analysis and XRD analysis, and FTIR spectroscopy in both the solid and gas phases, was carried out to investigate the correlation between the safety parameters, particle size distributions, and thermal and chemical properties of HA powders.

Overall, the present research presented holds significant environmental implications by addressing the potential of HA derived from biowastes. The conversion of biowaste into valuable HA not only contributes to mitigating the environmental impact and safety risks of waste disposal but also aligns with green chemistry and, therefore, with sustainable resource utilization objectives.

2. Experimental section

2.1. Materials

Humic Acid Sodium Salt (Aldrich_HA, purity ≥99.8%, CAS number: 68131–04–4) was purchased from Sigma-Aldrich (Milan, Italy). The average molecular weight is 226.14 g/mol.

Humic acid from Artichoke was extracted by composted Artichoke residues (Artichoke_HA), according to the procedure described elsewhere (Venezia et al., 2022b). The Artichoke residues were obtained in the composting facility of the Experimental Farm of University of Napoli Federico II at Castel-Volturno (CE).

Humic acid from compost (Compost_HA) was extracted by the compost supplied by Verde Vita (s.r.l, Sassari) following the procedure described elsewhere (Spaccini et al., 2019).

Briefly, 100 g of air-dried compost samples were suspended in 500 mL of 1 M NaOH solution in polypropylene containers and shaken overnight in a rotatory shaker. The mixture was centrifuged, and the supernatant was brought to acidic pH using 37 wt% HCl with 37 wt% HCl before being washed again. Humic acids refer to the fraction of compost that precipitates at pH 1. A part of this fraction was dialyzed until Cl-free against distilled water and freeze dried, to obtain CompostPD_HA (Spaccini et al., 2019). Compost_HA and CompostPD_HA were tested to show the effects of post-extraction treatments such as dialysis on the resilient or reactive character of the sample.

2.2. Methods

The flammable behavior of all samples was characterized through the Minimum Ignition Energy (MIE) and Layer Ignition Temperature (LIT) assessments using standard testing procedures (ASTM E2021-15, 2015; ASTM International, 2003).

The MIKE3 device was used for comparison purposes to estimate the ignition energy of dust samples (ASTM E2019-03, 2019). It consists of a vertical glass tube with a volume of 1.2 L. The bottom is made of stainless steel and is shaped to serve as a dust distributor. In the centre of the distributor there is a mushroom-shaped air nozzle with seven holes for air flow control and air delivery. Two tungsten electrodes (Diameter of 4 mm) are located at 1/3 height from the bottom of the test chamber and 6 mm spaced. The top of the test chamber is equipped with a hinged rotating disc (venting) that the explosion can open to discharge the explosion products and maintain the atmospheric pressure. The device can control both the spark energies by means of the release of the energy stored in a bank of capacitors of different capacities and the (ignition) delay time between the dust suspension (actuation of the release valve) and the triggering of the spark (the delay time affects the initial turbulence level). The delay time can be varied between 30 and 180 ms. In this work, a delay time of 120 ms with an inductance of 1 mH coupled to the capacitors circuit were used since in this condition the most conservative results were obtained. Each sample was subjected to a maximum of ten dispersions using during each series both a fixed concentrations and spark energy (ASTM International, 2003). For LIT measurements, the complete apparatus consists of a circular heated aluminium plate whose superficial temperature is controlled by a suitable PID controller. On the canter of this plate is placed the powder contained in a sample holder capable to form a layer of 5 mm of thickness (this is an aluminium ring of 100 mm of dimeter and 5 mm of height). During the experiments both the hot plate and the temperature measured at the center of the dusts layer are measured continuously. The LIT temperature is the lowest temperature for which no sign of reactivity (smoke generation, charring, glowing etc) is detected. The sample should be tested at different temperatures and left for at least 1 h to detect any temperature deviations from the temperature of the hot plate due to combustion reactions or visual events showing decomposition processes of the sample (ASTM E2021-15, 2015).

A laser diffraction granulometer Malvern Instruments Mastersizer 2000 was used to measure the granulometric distribution of dusts. The specific surface area (S_{BET}) was determined via N_2 adsorption at −196 °C starting from $P/P_0 = 5 \times 10^{-6}$ using a Quantachrome Autosorb-1C instrument (Quantachrome, Anton Paar Italia, Rivoli, Italy), after degassing the samples at 120 °C for 4 h.

The samples density was measured by using a pycnometer and ethanol as solvent and following the standard procedure (ASTM-D854, 2014). XRD experiments were carried out with a Malvern PANalytical diffractometer (Malvern, UK) with a nickel filter and Cu Kα radiation, to define the crystalline phases of HA samples.

FTIR analysis was carried out on all samples on solid and gases phase to investigate the functional groups of HA powders and the species generated during thermal treatment in inert as well as oxidative atmosphere. Nexus FTIR spectrometer equipped with a DTGS KBr (deuterated triglycine sulfate with potassium bromide windows) detector was used to perform. FTIR absorption spectra were recorded in the 4000-400 cm^{-1} range and with 2 cm^{-1} spectral resolution. All samples were prepared by mixing 200 mg of KBr and 1 mg of dried samples powders and pressing into pellets 13 nm in diameter. The spectrum of each sample was corrected for that of blank KBr.

To analyse gases produced from samples degradation, an FTIR gas was carried out through TGA/FTIR interface linked by transfer line to TGA furnace. The cell and transfer line of the TGA/FTIR interface were heated and kept at 220 °C. In this way, product gases from samples degradation could not condense. The output of this analysis is a Gram-Schmidt diagram. TG analysis were conducted to investigate the thermal behavior of samples by using a TA instrument simultaneous thermoanalyser SDT Q600 (TA Instrument, New Castle, DE, USA). Briefly, 10 mg of each sample were placed in a platinum pan and tested under both inert and oxidative atmosphere, in a temperature range between 25 and 1000 °C with a heating rate of 10 °C/min. The percentage in organic content in all samples was evaluated as following:

$$Organic\ content(\%) = \frac{W(200°C) - W(1000°C)}{W(200°C)} \cdot 100 \quad (2)$$

where W (200 °C) and W (1000 °C) are the weight at 200 °C and 1000 °C of the same sample, respectively. Moreover, the proximate analysis was carried out to assess the moisture, volatile, ash and fixed carbon contents by following the standard procedure (ASTM D5142 – 09, 2002).

Raman spectroscopy of the sampled materials was also performed using a Horiba XploRA Raman microscope system equipped with a 100× objective (NA 0.9, Olympus). The laser source was a frequency-doubled Nd:YAG laser ($\lambda = 532$ nm). The laser beam power, exposure time, and other instrumental parameters were selected to avoid structural changes in the sample due to thermal decomposition and to ensure the best resolution. Spectra were obtained at a laser beam power of approximately 0.1 mW and an accumulation (exposure) time of five cycles of 30 s each. For each sample, 10 spots were randomly selected and averaged to obtain statistically relevant Raman spectra (Vitiello et al., 2019).

3. Results and discussion

3.1. Flammable behavior

The flammability behavior was investigated through the measurement of LIT and MIE that quantify the sensitivity to ignition of a dust layer due to hot surface and of a dust cloud due to electric discharge, respectively. According to the results reported in Table 1, Artichoke_HA shows ignition susceptibility when in contact with the hot surface. Indeed, during LIT measurement on increasing temperature starting from 380 °C, browning, smoldering, and fracturing of the material disc were observed. Aldrich_HA is not susceptible to contact with hot surfaces, up to the 400 °C. Moreover, Artichoke_HA cloud is susceptible to the electric discharge with an ignition energy lower than 1000 mJ. Aldrich_HA is not susceptible to electric discharge, up to 1000 mJ. To understand the different flammability behavior, the samples physico-chemical characterization was carried out, to assess which of the following features account for different resilience: surface area, composition, granulometric distribution, crystal structure.

3.2. BET analysis

BET analysis was carried out to evaluate the specific surface area (SSA) of the samples. The adsorption isotherms for the HA samples show the typical trend of solids with a very low specific surface area, with small or negligible hysteresis, indication of low porosity. However, the most flammable sample (Artichoke_HA) shows the highest value of SSA (Table 1). In the flame propagation paths of a combustible dust (Di Benedetto and Russo, 2007), a larger SSA accelerates the preheating of the particle, promotes combustible-oxidant contact, accelerates the reaction in the heterogeneous phase and the devolatilization of the dust particles. Moreover, the density of the samples evaluated by means of a pycnometer is reported in Table 1. In terms of density, the analysed samples are comparable. It is worth noting that the density together with the diameter of the dust strongly affects the dispersibility of the dust.

3.3. Granulometric distribution

Laser diffraction granulometry was carried out to determine the size particles of the samples. As can be seen in Table 1 and Fig. 1, the most flammable sample is characterized by the highest values of mean,

Table 1
Flammable parameters, specific surface area, pore volume, density and granulometry of the samples.

	LIT (°C)	MIE (mJ)	SSA (m^2/g) (±0.05)	Pore volume BJH (cc/g) (±0.0005)	Density (g/m^3) (±0.1)	d (0.1) (μm)	d (0.5) (μm)	d (0.9) (μm)	D [3, 2] (μm)	D [4, 3] (μm)
Aldrich_HA	>400	>1000	0.58	0.007	1.26	0.57	5.56	22.66	0.70	9.32
Artichoke_HA	380	548	2.02	0.010	1.27	27.61	92.63	185.44	25.27	108.47

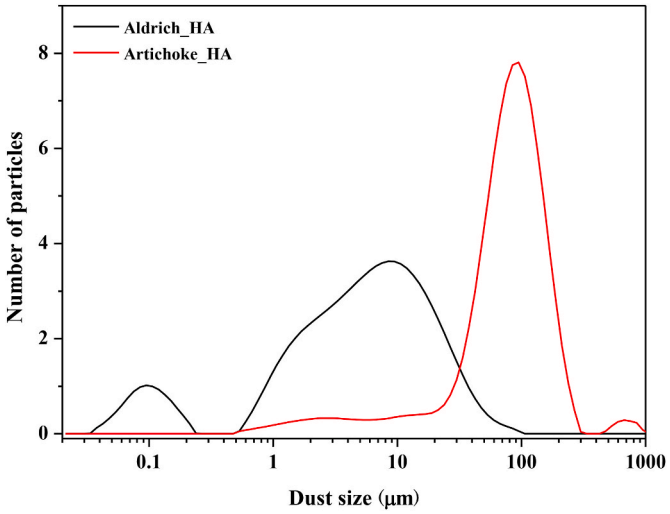

Fig. 1. Granulometric analysis.

volume weighted diameter, specific surface area and porosity. Consequently, the flammable behavior of Artichoke_HA cannot be attributed to its dust size but probably to its higher specific surface area and reactivity, the latter straight related to the nature and abundance of responsive functional groups.

3.4. FTIR analysis (solid phase)

In order to go deeper into reactive behavior of investigated HA, they were submitted to FT-IR analysis, to assess composition and identify the nature of available functional groups.

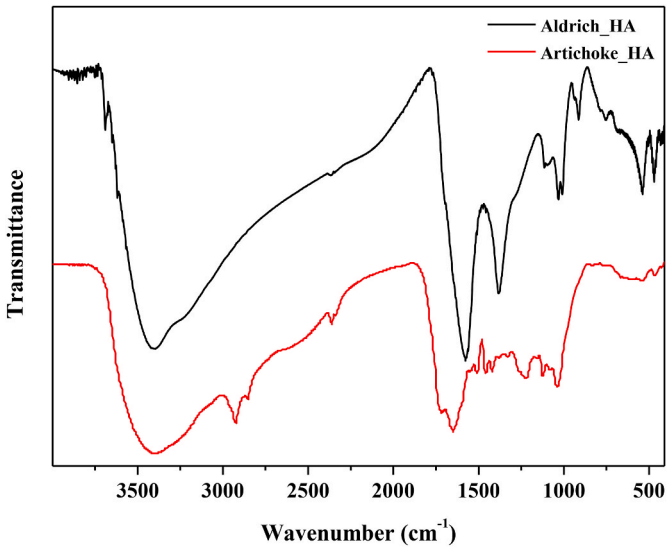

Fig. 2. FTIR spectra of the solid samples: Aldrich_HA (black line), Artichoke_HA (red line). (For interpretation of the references to colour in this figure legend, the reader is referred to the Web version of this article.)

FTIR spectra reported in Fig. 2 reveal the main characteristic bands, typical of HA, as described in Table 2. Aldrich_HA spectrum (Fig. 2, black spectrum) shows to main bands at around 1580 cm^{-1} and 1450 cm^{-1} and ascribable to COO- stretching vibration of carboxyl salt. On the other hand, the FTIR spectrum of Artichoke_HA (Fig. 2, red spectrum) shows additional bands at 2920 and 2850 cm^{-1} related to anti-symmetric and symmetric CH_2 stretching vibrations, respectively. Moreover, in the same spectrum other bands are clearly evident at 1730 cm^{-1} (C═C bond in aromatics and olefins, carboxyl C═O bond, ketone and quinone groups), 1506 cm^{-1} (ring vibration moieties of ortho-substituted aromatic compounds), 1458 cm^{-1} (OH of the phenols, COO– and –CH_3 bending vibration mode) and 1230 cm^{-1} (stretching vibration of C–O and C–O-R structures). On the other hand, these signatures are less intense or not significant in the FTIR spectrum of Aldrich HA, thus it can be inferred the presence of more reactive functional groups in HA Artichoke sample which may account for the higher flammability behavior shown in **Section 3.1**. Indeed, during the heating phase, the presence of more reactive functional groups can lead to a devolatilization with the production of flammable gases and/or heterogeneous reactions, even at low temperatures.

3.5. XRD analysis

XRD analysis was carried out to assess the crystallographic structure of the samples (Fig. 3), since it can strongly influence the flame propagation and the controlling step. Specifically, as reported by Di Benedetto and Russo (Di Benedetto and Russo, 2007), the flame propagation of a combustible dust can occur both in the homogeneous phase, through the devolatilization of the dust and the combustion of the produced flammable gases, and in the heterogeneous phase with the oxygen diffusion and heterogeneous combustion.

The XRD pattern of Aldrich_HA sample reveals the amorphous structure typical of HA, but also some diffraction peaks related to the presence of some inorganic materials, typical of clay soil (Marsh et al., 2019). Conversely, Artichoke_HA is characterized by a predominance of the amorphous fraction. It is worth noting that a lower crystalline degree promotes the oxygen diffusion that can sustain the combustion reaction thus supporting the flame propagation (Nabatame et al., 2003).

Although it is not possible to quantitatively measure the crystalline and amorphous phase fractions from XRD analyses, it is possible to state that Artichoke_HA due to a marked amorphous fraction with respect to

Table 2
FTIR band identification and assignments of HA samples.

Bands (cm^{-1})	Assignments
3700–3000	Phenolic –OH hydroxyl groups
3000–2800	Asymmetric and symmetric –CH_2 stretching
1760–1580	Antisymmetic COO^- Stretching Vibration of carboxyl salt, C=C bond in aromatics and olefins, carboxyl C=O bond, ketone and quinone groups
1510	Ring vibration modes of ortho-substituted aromatic compounds
1460–1380	OH of the phenols, COO– and –CH_3 bending vibration mode, symmetric COO^- Stretching Vibration of carboxyl salt
1280–1020	Stretching vibration of C–O and C–O-R structures
1040	Stretching vibration of C–N
1005	Stretching vibration of C–O
910	Out-of-phase bending vibration of aromatic C–H

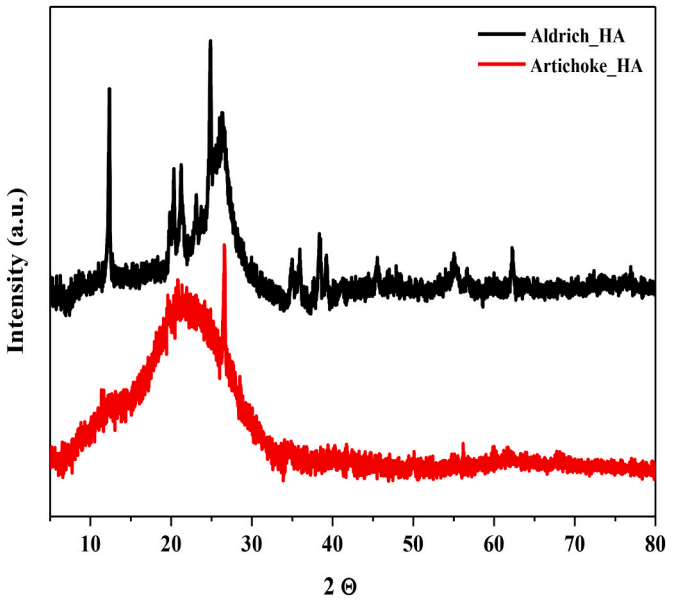

Fig. 3. XRD analysis of the samples: Aldrich_HA (black line), Artichoke_HA (red line). (For interpretation of the references to colour in this figure legend, the reader is referred to the Web version of this article.)

the other samples is characterized by a faster flame propagation in the heterogeneous phase when controlled by oxygen diffusion. This feature justifies the lower value of minimum ignition energy in comparison with the Aldrich_HA sample.

3.6. Thermogravimetric analysis (TGA) results

TGA provided crucial insights into how Aldrich_HA and Artichoke_HA samples behaved under varying temperature conditions, shedding light on their decomposition, stability, and thermal properties. Indeed, proximate analysis was performed on each sample in inert atmosphere to quantify the volatile (V), the humidity (M), the ash (A) and the fixed carbon (F) contents, following the standard procedure, reported elsewhere (ASTM D7582 - 15, 2015). The results in Table 3 show that Artichoke_HA is characterized by a higher amount of volatile content with respect to Aldrich_HA. Fig. 4 shows the TGA curves in inert atmosphere of both Adrich_HA and Artichoke_HA. Starting from the onset temperature of 214 °C, Artichoke_HA shows a continued weight loss until 600 °C, suggesting the greater reactivity also at lower temperature with respect to the other sample.

Aldrich_HA (black line), Artichoke_HA (red line)

To analyse the composition of the produced gases during devolatilization, FTIR on the gaseous phase was carried out (Fig. 5 and Table 4). Above all, Artichoke_HA releases flammable gaseous species (i.e. ammonia, hydrocarbons, carbon monoxide and isocyanic acid) at low temperature with the highest weight loss rate at 350 °C. These gases can take part to homogenous flame propagation of the samples. More specifically, Artichoke_HA heating in inert atmosphere leads to the generation of also isocyanic acid and hydrocarbon compounds. The larger amount of volatile species released by Artichoke_HA with respect to Aldrich_HA might be straight related to the higher abundance of reactive moieties in the former sample, as evidenced by FT-IR spectra. Finally, Aldrich_HA decomposes in CO_2 and H_2O under high temperatures with the highest weight loss rate at 500 °C.

To evaluate the interaction of the samples with oxygen, thermogravimetric analyses were also carried out in an oxidative atmosphere (Fig. 6). Also in this case, the samples showed a high weight loss during heating, even higher than the analysis in inert atmosphere, suggesting

Table 3
Proximate analysis of the samples (error ±1%) (ASTM D7582 - 15, 2015).

Sample	M%	V%	A%	F%
Aldrich_HA	8	37	24	31
Artichoke_HA	7	55	26	12

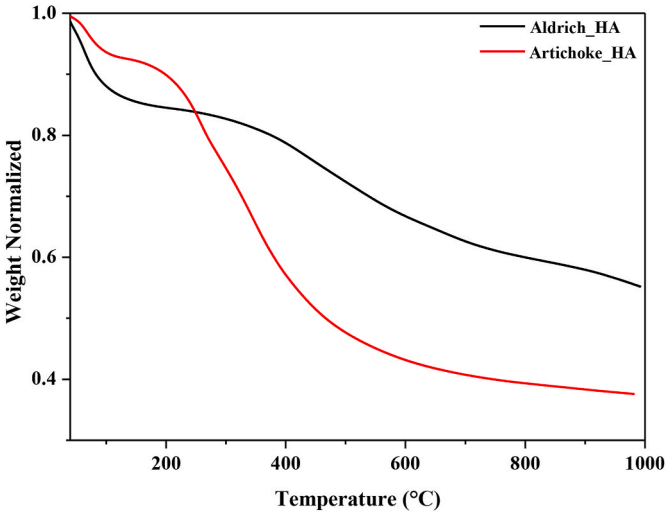

Fig. 4. TGA analysis in inert atmosphere of the samples.

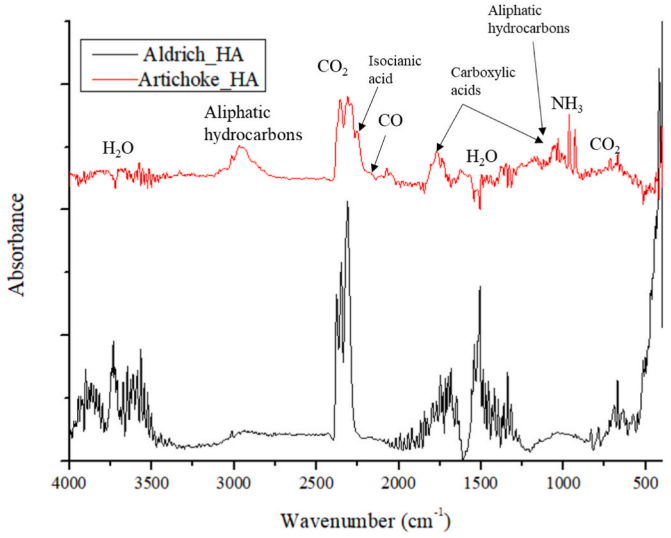

Fig. 5. FTIR analysis in the gaseous phase in inert atmosphere of the samples: Aldrich_HA (black line) and Artichoke_HA (red line). (For interpretation of the references to colour in this figure legend, the reader is referred to the Web version of this article.)

Table 4
Attribution of the FTIR gas peaks.

Gas species	Peak (cm^{-1})	Sample
Carbon dioxide	2400-2200 and 669	Aldrich_HA
Water	4000-3500 and 1750-500	Aldrich_HA
Ammonia	3330 and 1000-900	Artichoke_HA
Hydrocarbon chain	2934 and 2866	Artichoke_HA
Carbon monoxide	2180–2106	Artichoke_HA (trace)
Isocyanic acid	2250	Artichoke_HA
Carboxylic acids (e.g., formic acid)	1750	Artichoke_HA

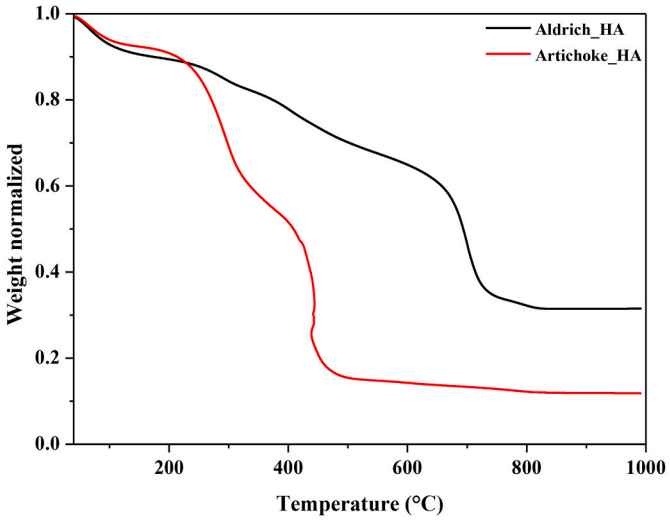

Fig. 6. TGA analysis in oxidative atmosphere of the samples: Aldrich_HA (black line) and Artichoke_HA (red line). (For interpretation of the references to colour in this figure legend, the reader is referred to the Web version of this article.)

that the samples interact with oxygen and possibly undergo heterogeneous flame propagation. As reported in Table 5, during the thermal heating in the presence of the oxidant, all species release CO_2 and H_2O, but their thermal trends are different from each other. Particularly, Aldrich_HA decomposes in CO_2 and H_2O, as well as in inert atmosphere. However, as can be seen in Fig. 7a, the curve in the oxidising environment deviates from the inert environment above 700 °C, indicating an interaction (combustion) of the solid with the oxygen active at high temperatures. Consequently, the final weight loss is greater in oxidative environment.

On the other hand, Artichoke_HA decomposes into CO_2 and H_2O in oxidative atmosphere, and thus showed a completely different behavior from that in an inert environment, where the gases produced were predominantly flammable. From the analysis of the thermal behavior in inert and oxidising atmosphere it can be inferred that these samples may undergo two types of flame propagation, homogeneous with the formation of combustible gases at low temperature and heterogeneous with the direct interaction of the solid with oxygen in the air. In the case of Artichoke_HA (Fig. 7b), the thermal behavior remains similar to that recorded in nitrogen, up to a temperature of 420 °C, suggesting that in this temperature range combustion must occur in the gas phase, involving produced volatiles. Then, at higher temperatures than 420 °C, a strong interaction with oxygen is triggered, leading to an additional weight loss of about 40%, which quickly ends at the offset temperature (500 °C).

Therefore, Artichoke_HA has a higher decomposition rate also in oxidative atmosphere than Aldrich_HA, reaching the weight loss plateau at 500 °C (Fig. 6). Obtained results are in accordance with higher flammability parameters (MIE and LIT) measured for Artichoke_HA.

3.7. Effect of dialysis treatment on thermal and physico-chemical behavior of Compost_HA

3.7.1. Flammable behavior and chemical physical characterization

The properties and the behavior of HA greatly depend on their extraction, fractionation and purification methods which strongly affect their reactivity and resilience degree (Saiz-Jimenez, 1996), as well as thevalorisation procedures. Indeed, these processes can yield HA with varying molecular weights, structures, and chemical compositions, all of which can influence their performance and resilience in different application fields.

In this work, an agri-food compost supplied by a Sardinian company has been considered as HA source and the effect of the post-extraction process, such as dialysis, on the HA resilience degree has been investigated. Compost_HA and CompostPD_HA are the extracted fractions of organic matter that have not undergone and have undergone, the dialysis process following the extraction procedure, respectively.

All the flammable and physico-chemical parameters are given in Table 6. Even if the Compost_HA before and after the dialysis process (CompostPD_HA) show the same SSA, pore volume and density values, CompostPD_HA becomes more prone to ignition due to hot surfaces and electrical spark and then more like the Artichoke_HA sample.

Table 5
Attribution of the FTIR gas peaks.

Volatile	Peak (cm^{-1})	Dust
Carbon dioxide	2400-2200 and 669	Aldrich_HA, Artichoke_HA
Water	4000-3500 and 1750-500	Aldrich_HA, Artichoke_HA

3.7.2. FTIR analysis

Fig. 8 and Table 2 show FTIR bands of all systems, including those of Compost_HA and Compost PD_HA. FTIR spectra of Aldrich_HA and Compost_HA are very similar and show two main bands at about 1600 and 1400 cm^{-1} due to the presence of COO^- stretching vibration of carboxyl salt. On the other hand, Artichoke_HA, Compost_HA and CompostPD_HA show two additional peaks at 2920 and 2850 cm^{-1} related to antisymmetric and symmetric CH_2 stretching vibrations, respectively. , Indeed, FTIR spectrum of Artichoke_HA looks very similar to that of CompostPD_HA. Indeed, both exhibit significant bands in the range between 1760 and 1000 $cm^{-1,}$ and ascribable to some functional groups, including C═C of aromatics and olefins, carboxyl C═O of ketone and quinone groups, OH of the phenols, and $–CH_3$ which are the most reactive functional moieties of these materials, in terms of both thermal and functional properties. These features denote a lower resilience degree for Artichoke_HA and CompostPD_HA samples, and may account for the flammability behavior shown in **Section 3.1**. Indeed, during the heating phase, their reactive functional groups can lead to a devolatilization with the production of flammable gases and/or heterogeneous reactions, even at low temperatures, as suggested FTIR analysis of produced gas result.

3.7.3. XRD analysis

XRD analysis was carried out to assess the structure of investigated samples and achieve an exhaustive view of flammability behavior. Fig. 9 shows XRD profiles of all systems, also including those of Compost_HA and CompostPD_HA powders.

The XRD pattern of Compost_HA (blue curve) corresponds to that of sodium chloride (NaCl) characterized by a face-centred cubic crystalline structure. The presence of NaCl is caused by the extraction process with which HA is produced starting from compost. Indeed, the compost sample was subjected to an alkali extraction by means of NaOH solution and subsequently the organic fraction soluble at higher pH values was brought to acidic pH by using HCl, as described in the experimental section.

On the other hand, since CompostPD_HA samples are obtained after a dialysis process until Cl-free against distilled water, XRD profile of CompostPD_HA powders does not show any relevant peak related to NaCl in XRD pattern (Fig. 9, green pattern), but rather evidences an amorphous structure very similar to that of Artichoke_HA sample (Fig. 9, red pattern), further supporting the close flammability behavior of these samples.

3.7.4. Thermogravimetric analysis (TGA) results

Proximate analysis was also performed on Compost_HA and CompostPD_HA samples in inert atmosphere to quantify and compare the volatile (V), the humidity (M), the ash (A) and the fixed carbon (F) contents of these samples with those of Aldrich_HA and Artichoke_HA

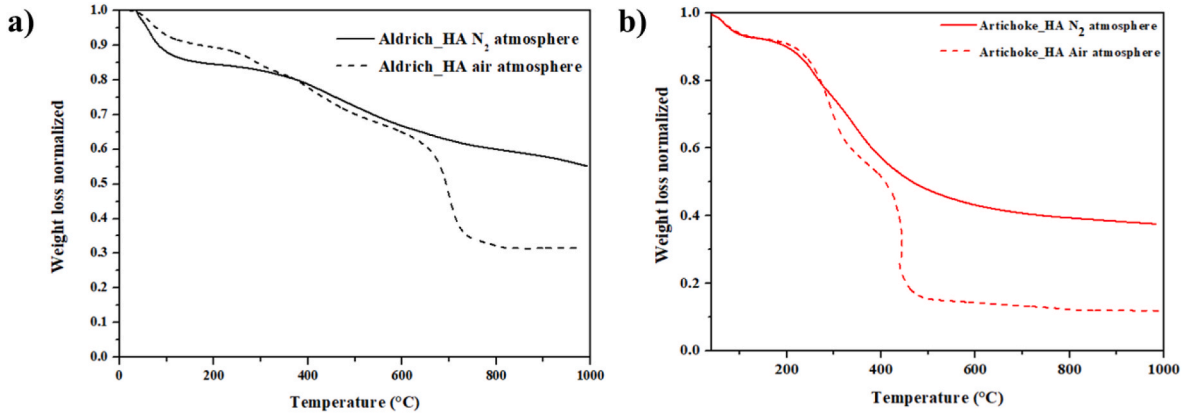

Fig. 7. TGA analysis in inert (solid line) and oxidative (dotted line) atmospheres of the samples: Aldrich_HA (a, black line) and Artichoke_HA (b, red line). (For interpretation of the references to colour in this figure legend, the reader is referred to the Web version of this article.)

Table 6
Flammable parameters, specific surface area, pore volume, density and granulometry of Compost_HA and CompostPD_HA samples.

	LIT (°C)	MIE (mJ)	SSA (m^2/g) (±0.05)	Pore volume BJH (cc/g) (±0.0005)	Density (g/m^3) (±0.1)	D [4, 3] (μm)
Compost_HA	>400	>1000	0.98	0.012	3.00	55.70
CompostPD_HA	380	740	1.10	0.017	3.00	53.10

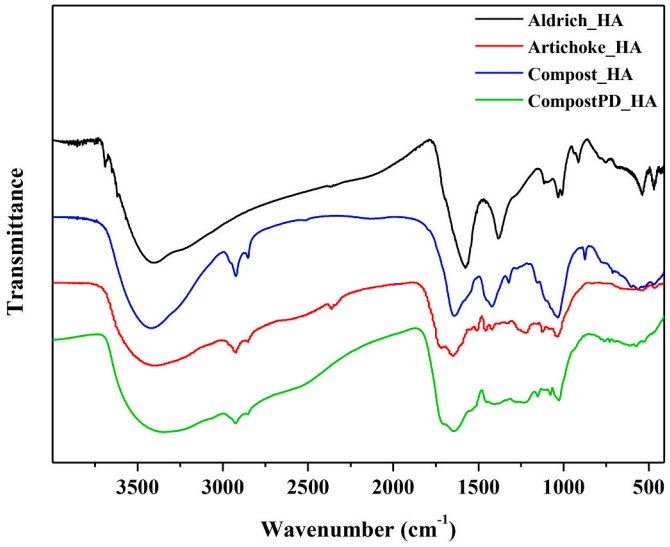

Fig. 8. FTIR analysis of samples: Aldrich_HA (black line), Artichoke_HA (red line), Compost_HA (blue line) and CompostPD_HA (green line). (For interpretation of the references to colour in this figure legend, the reader is referred to the Web version of this article.)

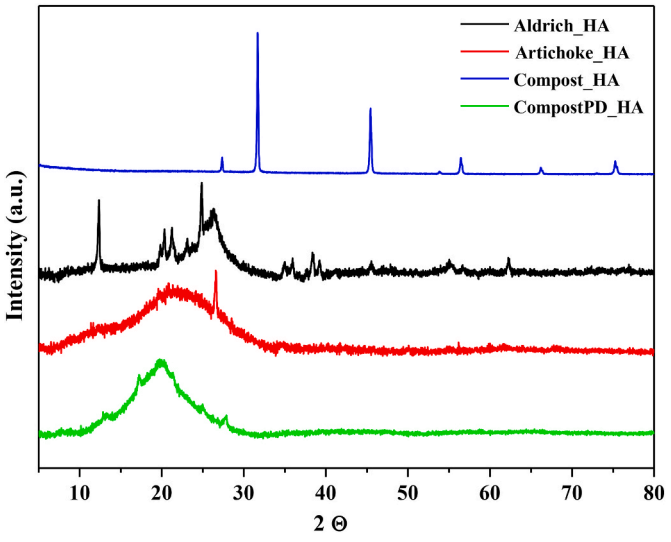

Fig. 9. XRD analysis of samples: Aldrich_HA (black line), Artichoke_HA (red line), Compost_HA (blue line) and CompostPD_HA (green line). (For interpretation of the references to colour in this figure legend, the reader is referred to the Web version of this article.)

ones, as described elsewhere (ASTM D7582 - 15, 2015).

Table 7 shows that Compost_HA is characterized by the highest amount of volatile content followed by Artichoke_HA and CompostPD_HA. In terms of moisture, the samples are comparable. It is worth noting that the amount of volatiles as well as their composition strongly affects the flame propagation paths that for organic dusts largely occurs in the homogeneous phase. This large volatile amount suggests the importance of analysing the concentration and the present species to assess the presence of flammable gases. The moisture (as well as the density and the diameter) strongly influences the flowability and the dispersibility of the samples but also the ignitability since the water works as heat sink.

Fig. 10 (a) shows TGA results of all systems in inert atmosphere,

Table 7
Proximate analysis of the samples (error ±1%) (ASTM D7582 - 15, 2015).

Sample	M%	V%	A%	F%
Aldrich_HA	8	37	24	31
Artichoke_HA	7	55	26	12
Compost_HA	5	64	24	7
CompostPD_HA	5	59	35	1

including those of HA extracted from the compost before and after the dialysis treatment (Compost_HA and CompostPD_HA).

It is possible to unveil how the final HA extraction treatment influences the thermal features of the obtained material. Indeed, the

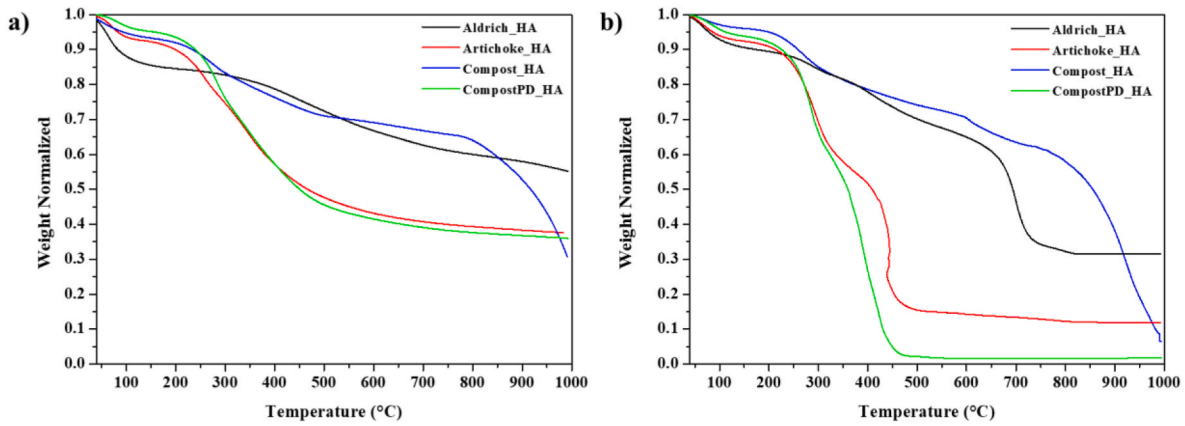

Fig. 10. TGA analysis of all systems in both inert (a) and oxidative atmosphere (b) of the samples: Aldrich_HA (black line), Artichoke_HA (red line), Compost_HA (blue line) and CompostPD_HA (green line). (For interpretation of the references to colour in this figure legend, the reader is referred to the Web version of this article.)

removal of NaCl salt through dialysis process makes the material "less thermally stable", causing it to behave much more like Artichoke_HA., both showing a weight loss of 60% with respect to the initial weight and degradation temperature of about 300 °C (Fig. 10a) and faster degradation kinetics. On the other side, Aldrich_HA and Compost_HA have a similar thermal trend until 800 °C, while at higher temperature the latter exhibits a slope change with a weight loss of about 34%.

In addition, the thermal degradation kinetic is higher for CompostPD_HA and Artichoke HA samples which show a degradation temperature of about 250–300 °C (Fig. 10 a).

Conversely, Compost_HA sample shows much slower thermal degradation kinetic with a consequential higher decomposition temperature (around 800 °C) a.

In an oxidative atmosphere (Fig. 10b), Aldrich_HA sample has the lowest weight loss, and the Compost_HA sample has similar decomposition kinetic up to about 700 °C, because itexhibits a higher degradation temperature (about 900 °C) On the other hand, the thermal properties of the Artichoke HA and CompostPD_HA samples appears quite similar even in an oxidising atmosphere, although CompostPD_HA sample has a higher weight loss (Table 7, Fig. 10 (b)). The results are in accordance with the similar flammability behavior recorded for both samples. Furthermore, since Compost_HA and CompostPD_HA simply differ for the presence of NaCl salt, gained results support the marked role played by a salt in determining the resilience for HA.

3.7.5. FT-IR gas

TGA analysis was coupled with FTIR on the gaseous phase in both oxidative and inert atmosphere on Compost_HA and CompostPD_HA to analyse and compare the composition of the produced gases during devolatilization with those of other analysed samples and go deeper into the mechanism of flame propagation. In inert atmosphere, Compost_HA releases some flammable gaseous species (i.e. hydrocarbons, carbon monoxide and carboxylic acids) ataround 350 °C, which represent the temperature with the highest weight loss weight (see Fig. 10 (a), blue curve). Conversely, CompostPD_HA behavior is much more similar to that of Artichoke_HA, since it releases additional flammable gaseous species, including ammonia and isocyanic acids.

In the oxidative atmosphere, both Compost_HA and CompostPD_HA decompose in CO_2 and H_2O under high temperatures with the highest weight loss rate at about 900 °C. Both of them show higher volatile amount with respect to Aldrich_HA, as also suggested by the proximate analysis results, even if the full decomposition is obtained at higher temperature.

3.7.6. Raman spectroscopy

In order to unveil the causes for the step-up of degradation, recorded at high temperature, Raman spectroscopy was carried out before and after degradation to obtain further chemical/structural information on the samples before and after the thermal treatment in inert atmosphere up 400 °C. This temperature was chosen starting from thermogravimetric results in inert atmosphere as a significative temperature for all the samples. Figs. 11 and 12 show the presence of two typical bands related to carbon materials, the so-called D peak and G peak (Commodo et al., 2017; Ferrari and Robertson, 2001). In particular, the former is centred at about 1380 cm^{-1} and it is associated with the presence of amorphous carbon , . Indeed, this bandis not observed in the Raman spectrum of highly crystalline graphite and graphene, whereas it becomes strong in nano-crystalline graphite, in defected and amorphous carbon. The slatteris centred at about 1570 cm^{-1} and it is Raman active for every sp^2 carbon networks (Commodo et al., 2017; Ferrari and Robertson, 2001). All samples present a photoluminescence background (PL) (Figs. 11 and 12), which is due to the radiative recombination of electrons and holes in the localized states generated by sp^2 clusters (Casiraghi et al., 2005).

Regarding the tested samples, all materials showed no significant differences among each other, since both the D and the G bands are present together with a strong PL background, even if they are not well defined (Fig. 11). On the other hand, the spectra acquired on the samples

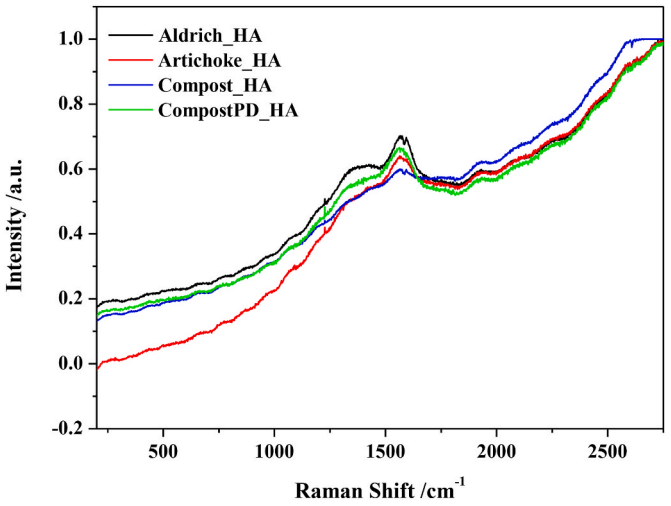

Fig. 11. Raman spectra of all samples: Aldrich_HA (black line), Artichoke_HA (red line), Compost_HA (blue line) and CompostPD_HA (green line). (For interpretation of the references to colour in this figure legend, the reader is referred to the Web version of this article.)

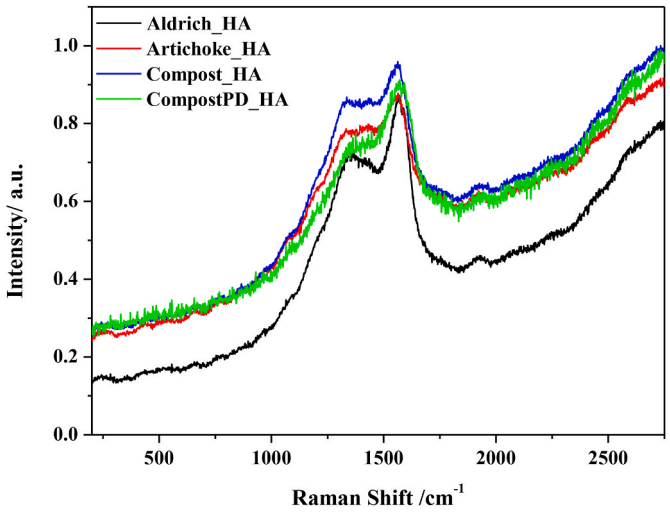

Fig. 12. Raman spectra of all samples after thermal treatment until 400 °C: Aldrich_HA (black line), Artichoke_HA (red line), Compost_HA (blue line) and CompostPD_HA (green line). (For interpretation of the references to colour in this figure legend, the reader is referred to the Web version of this article.)

after the thermal treatment until 400 °C shows some relevant differences (Fig. 12).

Indeed, in Aldrich_HA and Compost_HA samples the peaks related to disordered and graphitic carbon appeared well defined, suggesting that the samples had a higher amount of graphitic carbon after the thermal treatment. This can be related to the char production, which is bound to exert a protective action active as a barrier to oxygen diffusion, thus delaying degradation, in accordance with TG analysis results. On the other hand, Artichoke_HA and CompostPD_HA samples show not well-defined peaks, suggesting a lower amount of graphitic carbon after the thermal treatment, as previously predicted by TGA. Indeed, the thermal behavior suggested that these materials showed a higher weight loss even at lower temperature with a contextual generation of more flammable species (i.e., isocyanic acid and hydrocarbons).

4. Conclusions

Flammability, thermal and physico-chemical characterization of HA extracted from three different bio-residues allowed to assess their resilience degree (in terms devolatilization phenomena at lower temperatures and reactive functional groups), which represent a key parameter that should be assessed to set their effective valorisation practice. Experimental results suggested that flammability parameters strongly depend on the chemical nature, reactivity and on HA extraction process.

The most resilient HA composition can be exploited as functional bio-waste flame retardant additives for epoxy-based systems, because of their ability to promote the charring process during the epoxy degradation and establish good physical interactions with the polymer matrix. Aldrich_HA and Compost_HA belong to this category of materials.

Only by changing the type of extraction, a material can go from harmless behavior to massive production of volatiles when subjected to heating. This is the case of the sample CompostPD_HA, that after the dialysis process, tends to behave similarly to Artichoke_HA which appeared more susceptible to both hot surfaces and electrical discharges. For this kind of dusts, inertization is required and special safety measures should be taken for storage, handling, and use. Indeed, the storage tank should be equipped with temperature controls systems to prevent the activation of smoldering phenomena which can be ignition source of the dust cloud. However, these most reactive HA compositions can be explored as functional additives for polymeric materials to obtain multifunctional products with improved antioxidant and antimicrobial activity as well as higher mechanical performance. These properties, can make obtained HA-based polymeric materials good candidates for food packaging applications, protecting food quality from the destruction of heat, mechanical force, light, and oxidative free radicals.

The present work offers the opportunity to match the objectives of giving biowaste a new life according to their thermal, physico-chemical, and functional features.

Author contributions

Virginia Venezia: Conceptualization, Methodology, Investigation, Writing-original draft preparation. Maria Portarapillo: Conceptualization, Methodology, Investigation, Writing-original draft preparation. Gianluigi De Falco: Investigation, Writing-review and editing. Roberto Sanchirico: Writing-review and editing; Giuseppina Luciani: Conceptualization, Writing-review and editing, Supervision. Almerinda Di Benedetto: Conceptualization, Writing-review and editing, Supervision. All authors have read and agreed to the published version of the manuscript.

Declaration of competing interest

The authors declare that they have no known competing financial interests or personal relationships that could have appeared to influence the work reported in this paper.

Data availability

No data was used for the research described in the article.

Acknowledgements

The authors thank the Verde Vita company (s.r.l.) for providing the compost from which the humic acid HA was extracted. The authors thank the Department of Agricultural Science of University Federico II for providing Artichoke_HA. Authors acknowledge Mr. Andrea Bizzarro for his excellent technical support and for BET measurements. The authors thank Istituto di Scienze e Tecnologie per l'Energia e la Mobilità Sostenibili (STEMS), Consiglio Nazionale delle Ricerche for providing Raman spectroscopy instrument, laser diffraction granulometer, MIKE3 and LIT apparatus.

References

Afzal, M.Z., Yue, R., Sun, X.-F., Song, C., Wang, S.-G., 2019. Enhanced removal of ciprofloxacin using humic acid modified hydrogel beads. J. Colloid Interface Sci. 543, 76–83.

ASTM-D854, 2014. Standard Test Methods for Specific Gravity of Soil Solids by Water Pycnometer. ASTM International, West Conshohocken, PA. https://doi.org/10.1520/D0854-14.

ASTM D5142 – 09, 2002. Standard test methods for proximate analysis of the analysis sample of coal and. Methods. https://doi.org/10.1520/D5142-09.2.

ASTM D7582 - 15, 2015. Standard Test Methods for Proximate Analysis of Coal and Coke by Macro Thermogravimetric Analysis. ASTM Int. West, Conshohocken, PA.

ASTM E2019-03, 2019. Standard Test Method for Minimum Ignition Energy of a Dust Cloud in Air. ASTM Int., West Conshohocken, PA, pp. 1–9.

ASTM E2021-15, 2015. Standard Test Method for Hot-Surface Ignition Temperature of Dust Layers. ASTM Int. West Conshohocken, pp. 1–10.

ASTM International, 2003. Standard Test Method for Minimum Ignition Energy of a Dust Cloud in Air, pp. 1–11.

Casiraghi, C., Piazza, F., Ferrari, A.C., Grambole, D., Robertson, J., 2005. Bonding in hydrogenated diamond-like carbon by Raman spectroscopy. Diam. Relat. Mater. 14, 1098–1102.

Centrella, L., Portarapillo, M., Luciani, G., Sanchirico, R., Di Benedetto, A., 2020. Synergistic behavior of flammable dust mixtures: a novel classification. J. Hazard Mater. 397, 122784 https://doi.org/10.1016/j.jhazmat.2020.122784.

Commodo, M., Joo, P.H., De Falco, G., Minutolo, P., D'Anna, A., Gülder, Ö.L., 2017. Raman spectroscopy of soot sampled in high-Pressure diffusion flames. Energy Fuel. 31, 10158–10164. https://doi.org/10.1021/acs.energyfuels.7b01674.

Danzi, E., Di Benedetto, A., Sanchirico, R., Portarapillo, M., Marmo, L., 2021. Biomass from winery waste : evaluation of dust explosion hazards. Chem. Eng. Trans. 86, 301–306.

Danzi, E., Portarapillo, M., Di Benedetto, A., Sanchirico, R., Marmo, L., 2023. Ageing effect on ignition sensitivity of lignocellulosic dust. J. Loss Prev. Process Ind. 85, 105157. https://doi.org/10.1016/j.jlp.2023.105157.

de Melo, B.A.G., Motta, F.L., Santana, M.H.A., 2016. Humic acids: structural properties and multiple functionalities for novel technological developments. Mater. Sci. Eng. C 62, 967–974.

Di Benedetto, A., Russo, P., 2007. Thermo-kinetic modelling of dust explosions. J. Loss Prev. Process. Ind. 20, 303–309. https://doi.org/10.1016/j.jlp.2007.04.001.

Ferrari, A.C., Robertson, J., 2001. Resonant Raman spectroscopy of disordered, amorphous, and diamondlike carbon. Phys. Rev. B 64, 75414.

Ke, Y., Yang, X., Chen, Q., Xue, J., Song, Z., Zhang, Y., Madbouly, S.A., Luo, Y., Li, M., Wang, Q., Zhang, C., 2021. Recyclable and fluorescent epoxy polymer networks from Cardanol via solvent-free epoxy-Thiol chemistry. ACS Appl. Polym. Mater. 3, 3082–3092. https://doi.org/10.1021/acsapm.1c00284.

Liu, G., Shi, H., Kundu, C.K., Li, Z., Li, X., Zhang, Z., 2020. Preparation of novel biomass humate flame retardants and their flame retardancy in epoxy resin. J. Appl. Polym. Sci. 137, 1–12. https://doi.org/10.1002/app.49601.

Lowell, S., Shields, J.E., Thomas, M.A., Thommes, M., 2004. Characterisation of Porous Solids and Powders. Springer Netherlands. https://doi.org/10.1007/978-1-4020-2303-3.

Luo, X., Shen, L., Meng, F., 2019. Response of microbial community structures and functions of nitrosifying consortia to biorefractory humic substances. ACS Sustain. Chem. Eng. 7, 4744–4754.

Marsh, A., Heath, A., Patureau, P., Evernden, M., Walker, P., 2019. Phase formation behavior in alkali activation of clay mixtures. Appl. Clay Sci. 175, 10–21. https://doi.org/10.1016/j.clay.2019.03.037.

Muralidhara, A., Tosi, P., Mija, A., Sbirrazzuoli, N., Len, C., Engelen, V., De Jong, E., Marlair, G., 2018. Insights on thermal and fire hazards of humins in support of their sustainable Use in Advanced biorefineries. ACS Sustain. Chem. Eng. 6, 16692–16701. https://doi.org/10.1021/acssuschemeng.8b03971.

Nabatame, T., Yasuda, T., Nishizawa, M., Ikeda, M., Horikawa, T., Toriumi, A., 2003. Comparative studies on oxygen diffusion Coefficients for amorphous and γ-al2o3 films using 18O isotope. Japanese J. Appl. Physics, Part 1 regul. Pap. Short Notes Rev. Pap. 42, 7205–7208. https://doi.org/10.1143/jjap.42.7205.

Nuzzo, A., Mazzei, P., Drosos, M., Piccolo, A., 2020. Novel humo-Pectic hydrogels for controlled release of Agroproducts. ACS Sustain. Chem. Eng. 8, 10079–10088. https://doi.org/10.1021/acssuschemeng.0c01986.

Piccolo, A., 2002. The Supramolecular Structure of Humic Substances: a Novel Understanding of Humus Chemistry and Implications in Soil Science.

Portarapillo, M., Danzi, E., Guida, G., Luciani, G., Marmo, L., Sanchirico, R., Di Benedetto, A., 2022. On the flammable behavior of non-traditional dusts: dimensionless numbers evaluation for nylon 6,6 short fibers. J. Loss Prev. Process. Ind. 78, 104815 https://doi.org/10.1016/j.jlp.2022.104815.

Portarapillo, M., Danzi, E., Sanchirico, R., Marmo, L., Di Benedetto, A., 2021. Energy recovery from vinery waste: dust explosion issues. Appl. Sci. 11 https://doi.org/10.3390/app112311188.

Portarapillo, M., Luciani, G., Sanchirico, R., Di Benedetto, A., 2020. Ignition mechanism of flammable dust and dust mixtures: an insight through thermogravimetric/differential scanning calorimetry analysis. AIChE J. 66 https://doi.org/10.1002/aic.16256.

Portarapillo, M., Trofa, M., Sanchirico, R., Di Benedetto, A., 2021. CFD simulations of the effect of dust diameter on the dispersion in the 1 m3 explosion vessel. Chem. Eng. Trans. 86, 343–348. https://doi.org/10.3303/CET2186058.

Saiz-Jimenez, C., 1996. The chemical structure of humic substances: recent advances. Humic Subst. Terr. Ecosyst. 1–44.

Spaccini, R., Cozzolino, V., Di Meo, V., Savy, D., Drosos, M., Piccolo, A., 2019. Bioactivity of humic substances and water extracts from compost made by ligno-cellulose wastes from biorefinery. Sci. Total Environ. 646, 792–800.

Venezia, V., Avallone, P.R., Vitiello, G., Silvestri, B., Grizzuti, N., Pasquino, R., Luciani, G., 2022a. Adding humic acids to gelatin hydrogels: a way to Tune gelation. Biomacromolecules 23, 443–453. https://doi.org/10.1021/acs.biomac.1c01398.

Venezia, V., Matta, S., Lehner, S., Vitiello, G., Costantini, A., Gaan, S., Malucelli, G., Branda, F., Luciani, G., Bifulco, A., 2021. Detailed thermal, fire, and mechanical study of silicon-modified epoxy resin containing humic acid and other additives. ACS Appl. Polym. Mater. 3, 5969–5981.

Venezia, V., Pota, G., Silvestri, B., Vitiello, G., Di Donato, P., Landi, G., Mollo, V., Verrillo, M., Cangemi, S., Piccolo, A., 2022b. A study on structural evolution of hybrid humic Acids-SiO2 nanostructures in pure water: effects on physico-chemical and functional properties. Chemosphere 287, 131985.

Venezia, V., Verrillo, M., Gallucci, N., Di Girolamo, R., Luciani, G., D'Errico, G., Paduano, L., Piccolo, A., Vitiello, G., 2023. Exploiting bioderived humic acids: a molecular combination with ZnO nanoparticles leads to nanostructured hybrid interfaces with enhanced pro-oxidant and antibacterial activity. J. Environ. Chem. Eng. 11, 108973.

Vitiello, G., De Falco, G., Picca, F., Commodo, M., D'Errico, G., Minutolo, P., D'Anna, A., 2019. Role of radicals in carbon clustering and soot inception: a combined EPR and Raman spectroscopic study. Combust. Flame 205, 286–294. https://doi.org/10.1016/j.combustflame.2019.04.028.

Vitiello, G., Venezia, V., Verrillo, M., Nuzzo, A., Houston, J., Cimino, S., D'Errico, G., Aronne, A., Paduano, L., Piccolo, A., 2021. Hybrid humic acid/titanium dioxide nanomaterials as highly effective antimicrobial agents against gram (−) pathogens and antibiotic contaminants in wastewater. Environ. Res. 193, 110562.

Xu, B., Lian, Z., Liu, F., Yu, Y., He, Y., Brookes, P.C., Xu, J., 2019. Sorption of pentachlorophenol and phenanthrene by humic acid-coated hematite nanoparticles. Environ. Pollut. 248, 929–937.

Xu, C., Nasrollahzadeh, M., Selva, M., Issaabadi, Z., Luque, R., 2019a. Waste-to-wealth: biowaste valorization into valuable bio (nano) materials. Chem. Soc. Rev. 48, 4791–4822.

Xu, C., Nasrollahzadeh, M., Selva, M., Issaabadi, Z., Luque, R., 2019b. Waste-to-wealth: biowaste valorization into valuable bio(nano)materials. Chem. Soc. Rev. 48, 4791–4822. https://doi.org/10.1039/c8cs00543e.